seriously overestimating the velocities.
19. F. Gittes, B. Mickey, J. Nettleton, J. Howard, *J. Cell Biol.* **120**, 923 (1993); P. Venier, A. C. Maggs, M.-F. Carlier, D. Pantaloni, *J. Biol. Chem.* **269**, 13353 (1994); *ibid.* **270**, 17056 (1995); J. C. Kurz and R. C. Williams Jr., *Biochemistry* **34**, 13374 (1995); H. Felgner, R. Frank, M. Schliwa, *J. Cell Sci.* **109**, 509 (1996).
20. B. Mickey and J. Howard, *J. Cell Biol.* **130**, 909 (1995).
21. For 12 MTs, each over a 2-min interval, we measured the thermal fluctuations in the distance d between the middle of the MT and the line connecting the two ends of the MT: one end given by the position of the seed and the other end given by the position of the MT at length L, corresponding to the initial length of the MT (thus eliminating any sensitivity to changes in MT length during the measurement). An MT of length L can be viewed as two rigidly linked springs of length $L/2$, each with spring constant $24\kappa/L^3$. The total spring constant of this system is given by $48\kappa/L^3$. Given the equipartition theorem (*20*), the variance in d is connected to the flexural rigidity by

$$\kappa = k_B T L^3/[48\ \mathrm{var}(d)] \quad (7)$$

Using this formula, we found $\kappa = 34 \pm 7$ pN·μm² (mean ± SD). Errors in this number could arise from measurement errors in the position of the ends and the middle of the MT. This is especially true when measuring short MTs, in which case noise may lead to an underestimation of the rigidity. The 12 MTs varied from 10 to 20 μm in length. No length dependence of κ was apparent over this range, but MTs shorter than 10 μm produced lower values for κ.
22. T. L. Hill, *Linear Aggregation Theory in Cell Biology* (Springer-Verlag, New York, 1987).
23. C. S. Peskin, G. M. Odell, G. F. Oster, *Biophys. J.* **65**, 316 (1993).
24. The elastic restoring force of a MT that is slightly buckled against an immobile barrier is roughly equal to f_c (*14*). This is still true when the end of the MT moves a small distance (relative to the length of the MT) away from the barrier because of thermal fluctuations. The force driving the gap between the MT end and the barrier to zero is therefore independent of the size of the gap. To leave a gap of size δ in the direction of MT growth, the MT end must be displaced by a distance δ cos φ against the buckling force f, where φ is the angle between the force and the growth direction of the MT. This is equivalent to saying that the MT end must be displaced by a distance δ against the component of the force f_p that is directed parallel to the axis of the MT. The contact angle with the wall does not play any role because the direction of the force is determined by the shape of the buckled MT, not by the normal to the wall. The Brownian ratchet model for a MT that grows by bending perpendicular to its axis is described in A. Mogilner and G. Oster, *Biophys. J.* **71**, 3030 (1996).
25. D. N. Drechsel, A. A. Hyman, M. H. Cobb, M. W. Kirschner, *Mol. Biol. Cell* **3**, 1141 (1992).
26. This does not exclude, of course, the possibility that force affects both rates. For instance, a fit to the function

$$v(f_p) = A \exp(-0.5Cf_p/\kappa) - B \exp(0.5Cf_p/\kappa) \quad (8)$$

($q = 0.5$) produces a reasonable result as well: $\chi^2 = 0.43$ with $A = 1.20 \pm 0.05$ μm min⁻¹, $B = -0.007 \pm 0.010$ μm min⁻¹, and $C = 34 \pm 4$ μm². Note, however, that B is much smaller than A, implying that the effect of force is in any case dominated by a decrease in the on-rate, a result that is obtained for every positive value of q.
27. M. Dogterom, M.-A. Félix, C. C. Guet, S. Leibler, *J. Cell Biol.* **133**, 125 (1996).
28. A. A. Hyman, K. Middleton, M. Centola, T. J. Mitchison, J. Carbon, *Nature* **359**, 533 (1992).
29. T. E. Holy, M. Dogterom, B. Yurke, S. Leibler, *Proc. Natl. Acad. Sci. U.S.A.* **94**, 6228 (1997).
30. We thank T. E. Holy, S. Leibler, and K. Svoboda for discussions; K. Baldwin, T. E. Holy, and A. N. Pargellis for technical help; B. Shraiman and K. Svoboda for critical reading of the manuscript; and S. Leibler for use of his lab to prepare tubulin and MT seeds.

17 June 1997; accepted 17 September 1997

IKK-1 And IKK-2: Cytokine-Activated IκB Kinases Essential for NF-κB Activation

Frank Mercurio,* Hengyi Zhu, Brion W. Murray, Andrej Shevchenko, Brydon L. Bennett, Jian wu Li, David B. Young, Miguel Barbosa, Matthias Mann,

Anthony Manning, Anjana Rao

Activation of the transcription factor nuclear factor kappa B (NF-κB) is controlled by sequential phosphorylation, ubiquitination, and degradation of its inhibitory subunit IκB. A large multiprotein complex, the IκB kinase (IKK) signalsome, was purified from HeLa cells and found to contain a cytokine-inducible IκB kinase activity that phosphorylates IκB-α and IκB-β. Two components of the IKK signalsome, IKK-1 and IKK-2, were identified as closely related protein serine kinases containing leucine zipper and helix-loop-helix protein interaction motifs. Mutant versions of IKK-2 had pronounced effects on RelA nuclear translocation and NF-κB–dependent reporter activity, consistent with a critical role for the IKK kinases in the NF-κB signaling pathway.

Transcription factors of the NF-κB Rel family are critical regulators of genes that function in inflammation, cell proliferation, and apoptosis (*1*). The prototype member of the family, NF-κB, is composed of a dimer of p50 (NF-κB1) and p65 (RelA) (*2*). NF-κB exists in the cytoplasm of resting cells but enters the nucleus in response to various stimuli, including viral infection, ultraviolet irradiation, and proinflammatory cytokines such as tumor necrosis factor α (TNF-α) and interleukin-1 (IL-1) (*1*, *3*).

Activation of NF-κB is controlled by an inhibitory subunit, IκB, which retains NF-κB in the cytoplasm (*4*). NF-κB activation requires sequential phosphorylation, ubiquitination, and degradation of IκB as well as consequent exposure of a nuclear localization signal on NF-κB (*5*). Ser^{32} and Ser^{36} of IκB-α, and the corresponding Ser^{19} and Ser^{23} of IκB-β, represent critical phosphorylated residues (*6*). The IκB kinase shows a high degree of specificity for these residues, because an IκB-α variant in which Ser^{32} and Ser^{36} were substituted by Thr (S32T, S36T) showed much reduced phosphorylation and degradation in stimulated cells and interfered with endogenous NF-κB activation (*6*).

To identify the IκB kinase responsible for the initial critical step of NF-κB activation, we fractionated whole-cell extracts (WCEs) from TNF-α–stimulated HeLa cells by standard chromatographic methods (*7*). We assayed IκB kinase activity in each fraction by phosphorylating glutathione-S-transferase (GST)–IκB-α (1–54) or GST–IκB-β (1–44) (*8*). Kinase specificity was established by using (S32T, S36T) mutant GST–IκB-α (1–54) [GST–IκB-α (1–54; S32T, S36T)], and GST–IκB-β (1–44), in which Ser^{19} and Ser^{23} were mutated to Ala [GST–IκB-β (1–44; S19A, S23A)] (*8*). IκB kinase activity was not observed in unstimulated cell extracts but was strong in cells stimulated for 5 to 7 min with TNF-α (*9*). Gel-filtration chromatography resolved this IκB kinase activity in a broad peak of 500 to 700 kD (Fig. 1A). In contrast to the 600-kD IκB kinase complex that was observed after treatment of cell extracts with either okadaic acid or ubiquitin-conjugating enzymes (*10*), the IκB kinase activity described here displayed no requirement for ubiquitination (*9*). We refer to the protein complex that contains the inducible IκB kinase activity as the IKK signalsome.

NF-κB activation occurs under conditions that also stimulate mitogen-activated protein kinase (MAP kinase) pathways (*11*). We tested preparations containing the IKK signalsome for the presence of proteins associated with MAP kinase and phosphatase cascades (Fig. 1B). The MAP kinase kinase–1 (MEKK-1) and two Tyr-phosphorylated proteins of ~55 and ~40 kD copurified with IκB kinase activity (Fig. 1B). A protein of ~50 kD that reacted with an antibody to MAP kinase phosphatase–1 (anti–MKP-1) also copurified with the IκB kinase through several purification steps.

F. Mercurio, H. Zhu, B. W. Murray, B. Bennett, J. Li, D. Young, M. Barbosa, A. Manning, Signal Pharmaceuticals, Inc., 5555 Oberlin Drive, San Diego, CA 92121, USA.
A. Shevchenko and M. Mann, European Molecular Biology Laboratory, Meyerhofstrasse 1, D-69012 Heidelberg, Germany.
A. Rao, Center for Blood Research and the Department of Pathology, Harvard Medical School, 200 Longwood Avenue, Boston, MA 02115, USA.

*To whom correspondence should be addressed. E-mail: fmercuri@signalpharm.com

We examined antibodies against proteins copurifying with the IKK signalsome activity for their ability to immunoprecipitate IκB kinase activity. Of a panel of antibodies tested, one of three anti–MKP-1 efficiently coimmunoprecipitated an inducible IκB kinase activity from HeLa cells (*12*) and primary human umbilical vein endothelial cells (HUVECs) (*9*). IκB kinase activity was not detected in immunoprecipitates from unstimulated HeLa cells, but it was detected within minutes of exposure of cells to TNF-α (Fig. 2A). This IκB

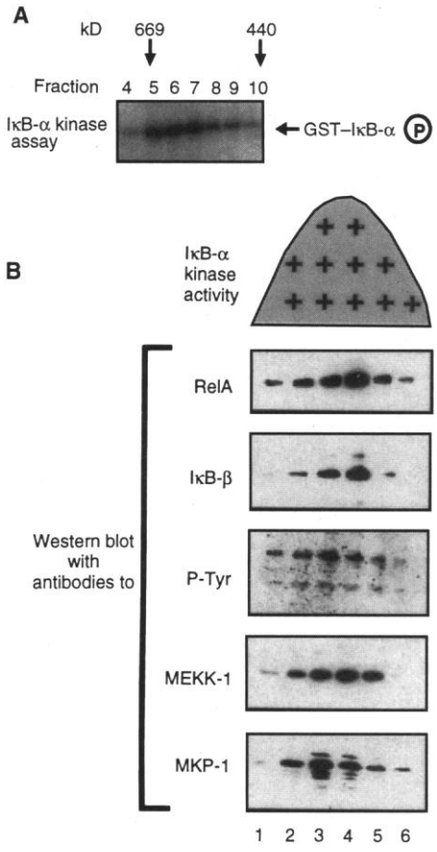

Fig. 1. Identification of the IKK signalsome. (**A**) IκB-α kinase activity chromatographs as a large complex (500 to 700 kD). WCE of TNF-α–stimulated (20 ng/ml; 7 min) HeLa S3 cells was prepared, fractionated on a Superdex 200 gel-filtration column, and monitored for IκB-α kinase activity (*8*). Phosphorylation of the GST–IκB-α (1–54) WT substrate is indicated by arrow on the right. Molecular mass standards are indicated by arrows on top. (**B**) Identification of proteins that cochromatograph with the IKK signalsome. IKK signalsome was partially purified from extracts of TNF-α–stimulated HeLa S3 cells by sequential fractionation on Q Sepharose, Superdex 200 gel-filtration, Mono Q, and phenyl Superose columns. Phenyl Superose fractions containing the peak of IKK signalsome activity were subjected to Western blot analysis with several different antibodies, indicated on the left. The relative level of IKK signalsome activity is indicated by the number of plus signs in upper shaded area.

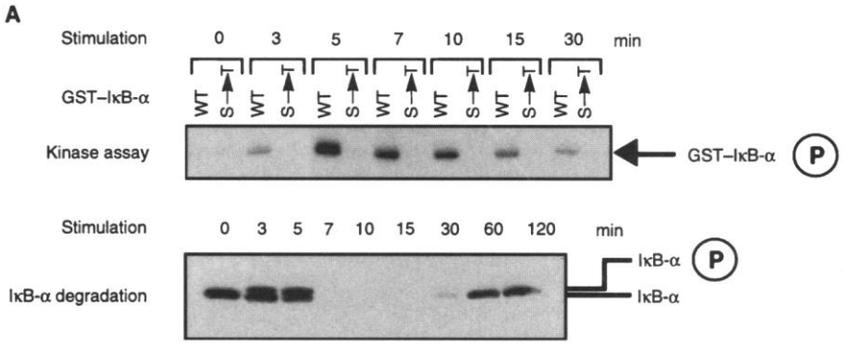

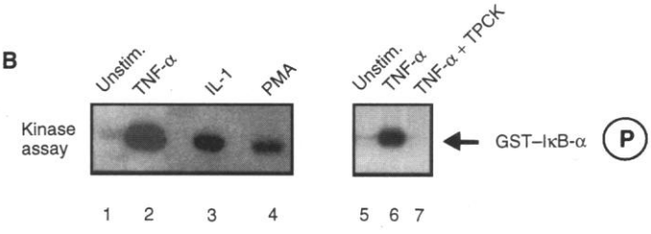

Fig. 2. Biochemical properties of IKK signalsome activity immunoprecipitated by anti–MKP-1. (**A**) Increased activity of IKK signalsome after cell stimulation. (**Upper**) Time course for increased IKK signalsome activity. Anti–MKP-1 immunoprecipitates from extracts of HeLa S3 cells stimulated with TNF-α (20 ng/ml) for the indicated times were assayed for 1 hour by a standard immune complex kinase assay. Either GST–IκB-α (1–54) WT or the GST–IκB-α (1–54; S32T, S36T) mutant (S→T) (4 μg) was used as substrate. (**Lower**) IκB-α phosphorylation and degradation kinetics. HeLa cell extracts prepared as described in the upper panel were examined by protein immunoblotting for IκB-α degradation. IκB-α supershifting, a result of stimulus-dependent phosphorylation, is observed after 3 and 5 min of stimulation followed by the disappearance of IκB-α. (**B**) Stimulus-dependent activation of IKK signalsome is blocked by TPCK. Anti–MKP-1 immunoprecipitates from cell extracts of HeLa S3 cells stimulated for 7 min with TNF-α (20 ng/ml; lanes 2 and 6), IL-1 (10 ng/ml; lane 3), or PMA (50 ng/ml; lane 4), or treated for 30 min with TPCK (15 μM; lane 7) before stimulation with TNF-α, were examined for IKK signalsome activity. GST–IκB-α (1–54) WT (4 μg) was used as substrate. (**C**) The IKK signalsome phosphorylates Ser^{32} and Ser^{36} of IκB-α. (**Upper**) IκB-α (21–41) peptides that were unphosphorylated or that had been synthesized with P-Ser at position 32 or 36 were enzymatically phosphorylated by the IKK signalsome with [γ-^{32}P]ATP. The unrelated c-Jun (56–70), c-Jun (65–79), and MKP-1 (349–366) peptides functioned as poor substrates for the IKK signalsome. (**Lower**) The same set of substrates described for the upper panel were subjected to enzymatic phosphorylation by JNK2 with [γ-^{32}P]ATP used as a control. Specific peptide substrates used are indicated on top. Source of the kinase is indicated on the left. Molecular mass standards (in kilodaltons) are indicated on the right. (**D**) The IKK signalsome specifically phosphorylates Ser^{32} and Ser^{36} of the IκB-α protein and RelA in the context of a RelA–IκB-α complex. Anti–MKP-1 immunoprecipitates from cell extracts of HeLa S3 cells stimulated with TNF-α (20 ng/ml; 7 min) were examined for their ability to phosphorylate recombinant RelA–IκB-α complex containing either WT IκB-α (lane 3) or IκB-α (S32A, S36A) mutant (lane 4) protein. Specific substrates used are indicated on top. Positions of phosphorylated substrates are indicated by arrows on the left.

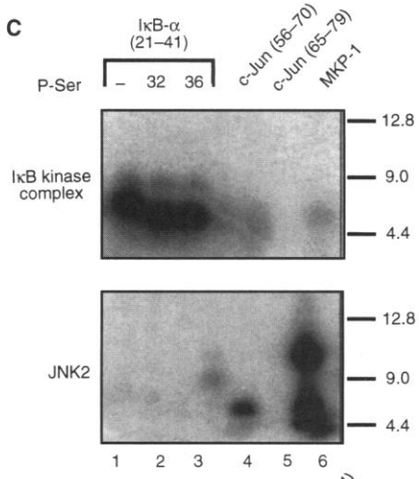

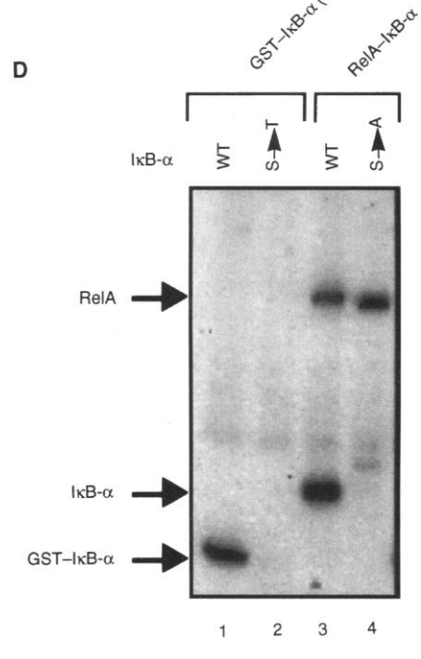

kinase did not phosphorylate GST–IκB-α (1–54; S32T, S36T). IκB-α kinase activity was maximal by 5 min and declined thereafter, consistent with the time course of IκB-α phosphorylation and degradation (Fig. 2A). Kinase activity was also induced by stimulation of cells with IL-1 or phorbol 12-myristate 13-acetate (PMA) (Fig. 2B); moreover, no increase in activity was detected from HeLa cells treated with *N*-tosyl-L-phenylalanine chloromethyl ketone (TPCK), an inhibitor of NF-κB activation (6), before cell stimulation with TNF-α.

We established the substrate specificity of the IKK signalsome by using various peptides and recombinant proteins (*8*, *13*). The kinase was capable of phosphorylating an IκB-α (21–41) peptide as well as two additional IκB-α (21–41) peptides, each bearing an unmodified Ser at position 32 or 36 and phosphoserine (P-Ser) at the other position (Fig. 2C). An IκB-α (21–41) peptide bearing Thr at both positions was phosphorylated <one-tenth as well as wild-type (WT) peptide, whereas an IκB-α (21–41) peptide bearing P-Ser at both positions was not phosphorylated at all (9). The IKK signalsome did not phosphorylate two c-Jun peptides containing Ser^{63} and Ser^{73}, respectively, or an MKP-1 peptide containing four Ser and three Thr (Fig. 2C). The latter peptides were substrates for JNK2. These experiments indicate that Ser^{32} and Ser^{36} were both specifically phosphorylated by the IKK signalsome.

The IKK signalsome phosphorylated WT IκB-α but not IκB-α (S32A, S36A) in the context of a physiological RelA–IκB-α complex (Fig. 2D). GST–IκB-β (1–44) was

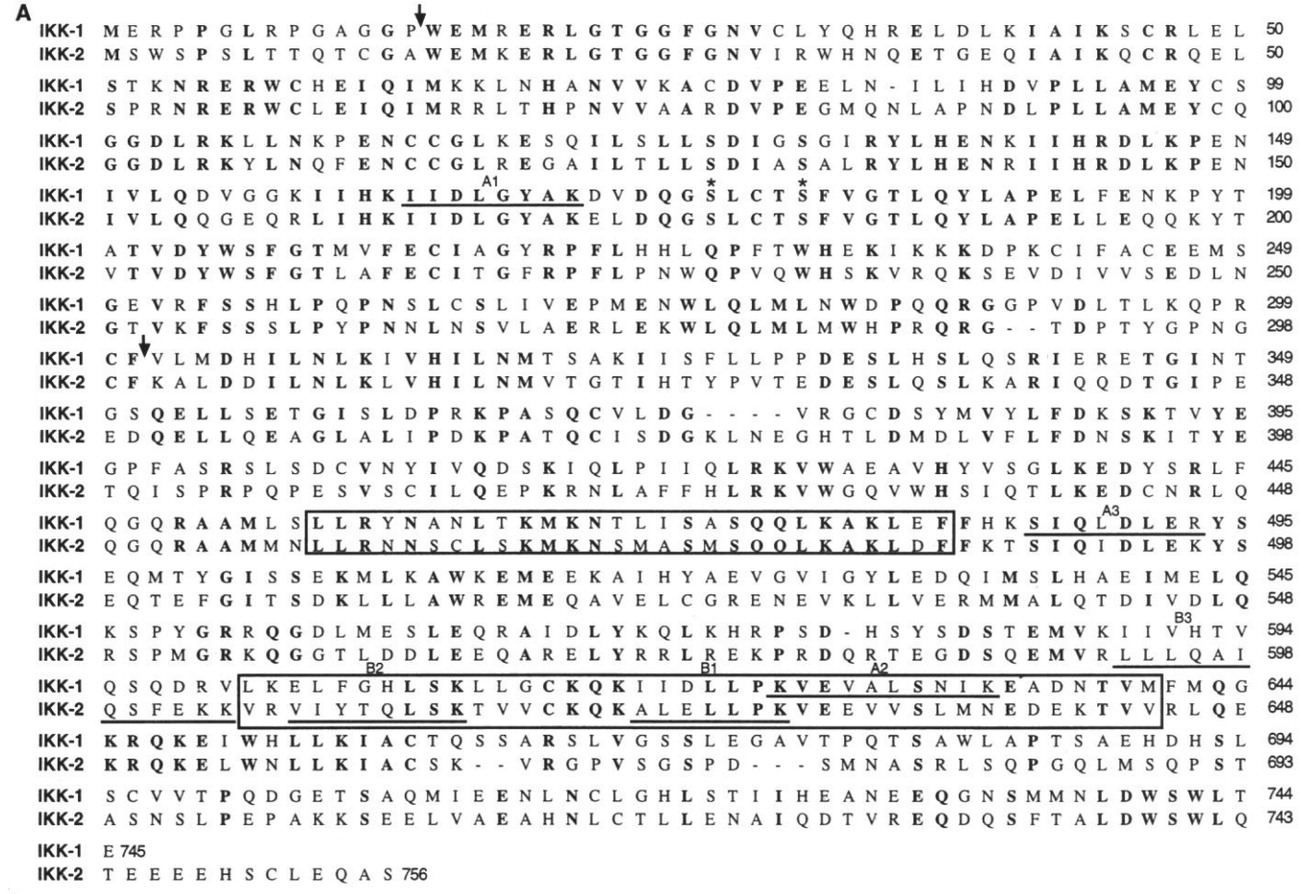

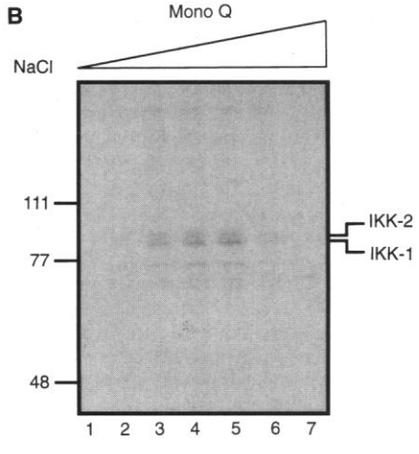

Fig. 3. Purification and cloning of IKK-1 and IKK-2. (**A**) Amino acid sequence comparison of human IKK-1 and IKK-2. Arrows, boundaries of the kinase domain; underlining, peptide sequences identified by nanoelectrospray mass spectrometry; boldface, amino acid identities conserved between IKK-1 and IKK-2; asterisks, amino acid identity to a region conserved among the MEK family of protein kinases demonstrated to be essential for stimulus-dependent activation; NH_2-terminal boxed area, leucine zipper motif; COOH-terminal boxed area, helix-loop-helix domain; dashes, gaps inserted to optimize alignment. (**B**) Purified IKK signalsome fractions contain two prominent bands at 85 and 87 kDa. WCE was prepared from TNF-α–stimulated (20 ng/ml; 7-min induction) HeLa S3 cells (1.2 g of total protein). The IKK signalsome was immunoprecipitated from the HeLa S3 WCE with anti–MKP-1 antibodies, washed with buffer containing 3.5 M urea, and eluted overnight with excess MKP-1–specific peptide. Eluted IKK signalsome was subjected to Mono Q chromatography. Fractions containing active IKK signalsome activity were subjected to SDS-PAGE, and protein bands were visualized by a standard silver staining protocol. Peak IKK signalsome activity is associated with lanes 3, 4, and 5. Protein bands corresponding to IKK-1 and IKK-2 are indicated on the right. Molecular mass standards (kD) are indicated on the left.

also phosphorylated, albeit with lower affinity; the K_m for IκB-β was tenfold higher than the K_m for IκB-α (9). The IKK signalsome also contained a strong RelA kinase activity that was distinct from the IκB kinase activity in that it was dissociated from the IKK signalsome by rigorous washing (9). No activity toward several other substrates was observed, including myelin basic protein (MBP), GST–activation transcription factor–2 (ATF2) (1–112), GST–c-Jun (1–79), GST–extracellular signal regulated kinase (ERK3), GST–Elk-1 (307–428), GST-p38, and a GST fusion protein containing the COOH-terminal region of IκB-α (242–314) (9).

We developed a two-step IKK signalsome purification method. Proteins from whole-cell lysates of TNF-α–stimulated HeLa cells were immunoprecipitated with anti–MKP-1. We eluted the IKK signalsome with an MKP-1 peptide and fractionated it further by anion-exchange chromatography (*14*). Fractions with IκB kinase activity were pooled and subjected to preparative SDS gel electrophoresis. Two prominent protein bands of 85 and 87 kD (designated IKK-1 and IKK-2, respectively, in Fig. 3B) correlated with the peak of IκB kinase activity. The 85- and 87-kD bands were excised, digested with trypsin, and analyzed by high mass accuracy matrix-assisted laser deposition and ionization (MALDI) peptide mass mapping (*15*, *16*). The 85-kD band was identified as CHUK (conserved helix-loop-helix ubiquitous kinase) (*17*), whereas the 87-kD band was not found in a comprehensive database. Three peptides derived from the 87-kD band were sequenced by nanoelectrospray tandem mass spectrometry (*18*) and found as identical matches to human expressed sequence tag (EST) clones (*15*) that were similar to human and mouse CHUK (*17*). Once the complete coding sequence of IKK-2 was obtained (*19*), all sequenced peptides (apart from two peptides derived from IKK-1) could be assigned to this protein (Fig. 3A).

Sequence analysis revealed that IKK-1 and IKK-2 are related protein serine kinases (51% identity) containing protein interaction motifs (Fig. 3A). Both contain the kinase domain at the NH_2-terminus with a leucine zipper motif and a helix-loop-helix motif in the COOH-terminal region. Northern blot analysis indicated that mRNAs encoding IKK-2 were widely distributed in hu-

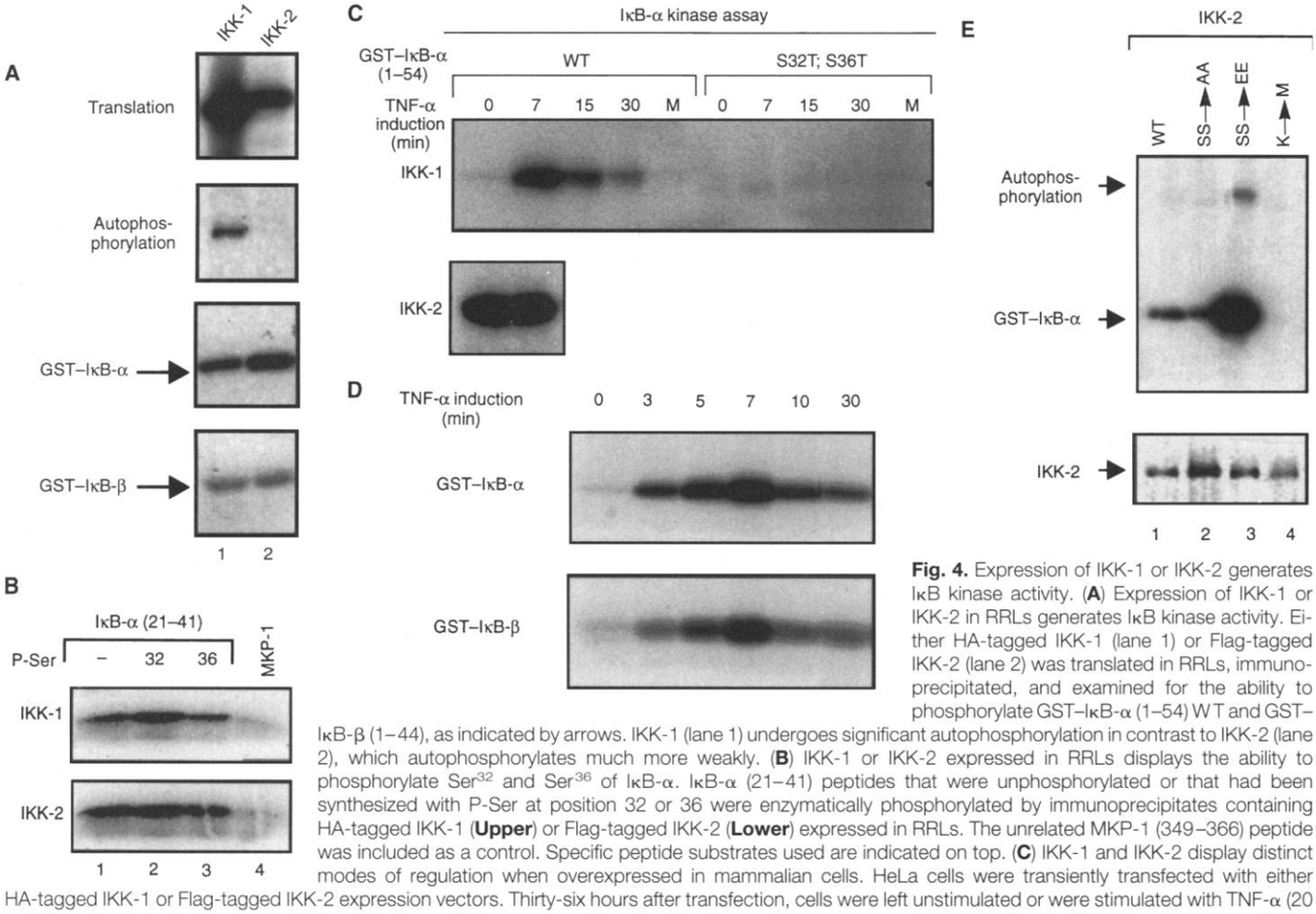

Fig. 4. Expression of IKK-1 or IKK-2 generates IκB kinase activity. (**A**) Expression of IKK-1 or IKK-2 in RRLs generates IκB kinase activity. Either HA-tagged IKK-1 (lane 1) or Flag-tagged IKK-2 (lane 2) was translated in RRLs, immunoprecipitated, and examined for the ability to phosphorylate GST–IκB-α (1–54) WT and GST–IκB-β (1–44), as indicated by arrows. IKK-1 (lane 1) undergoes significant autophosphorylation in contrast to IKK-2 (lane 2), which autophosphorylates much more weakly. (**B**) IKK-1 or IKK-2 expressed in RRLs displays the ability to phosphorylate Ser^{32} and Ser^{36} of IκB-α. IκB-α (21–41) peptides that were unphosphorylated or that had been synthesized with P-Ser at position 32 or 36 were enzymatically phosphorylated by immunoprecipitates containing HA-tagged IKK-1 (**Upper**) or Flag-tagged IKK-2 (**Lower**) expressed in RRLs. The unrelated MKP-1 (349–366) peptide was included as a control. Specific peptide substrates used are indicated on top. (**C**) IKK-1 and IKK-2 display distinct modes of regulation when overexpressed in mammalian cells. HeLa cells were transiently transfected with either HA-tagged IKK-1 or Flag-tagged IKK-2 expression vectors. Thirty-six hours after transfection, cells were left unstimulated or were stimulated with TNF-α (20 ng/ml) for the indicated times. Activities of the tagged kinases were determined by immunokinase assays with GST–IκB-α (1–54) WT or GST–IκB-α (1–54; S32T, S36T) used as substrate. The transfected kinase is indicated on the left. (**D**) Endogenous IKK-1 and IKK-2 display activation kinetics identical to the IKK signalsome activity. Endogenous IKK-1 and IKK-2 were immunoprecipitated, with antibodies directed against IKK-1 and IKK-2, from HeLa WCEs prepared from cells that were left unstimulated or that were stimulated with TNF-α (20 ng/ml) for the indicated times. The immunocomplexes were then subjected to standard kinase assays with GST–IκB-α (1–54) WT or GST–IκB-β (1–44) WT as substrate, as indicated on the left. (**E**) A constitutively active version of IKK-2 is generated by (S177E, S181E) mutations in the activation loop resembling those of the MEK family kinases. (**Upper**) Flag-tagged IKK-2 WT (lane 1), (S177A, S181A) (lane 2), (S177E, S181E) (lane 3), and K44M (lane 4) were translated in RRLs, immunoprecipitated with anti-Flag, and examined for their ability to phosphorylate GST–IκB-α (1–54) WT. Phosphorylated GST–IκB-α (1–54) and autophosphorylated IKK-2 are indicated with an arrow on the left. IKK-2 mutants are indicated at the top. (**Lower**) An equal portion of each immunocomplex, as indicated in the upper panel, was subjected to Western blot analysis with anti-Flag to establish relative levels of IKK-2 protein expression.

man tissues, with transcript sizes of about 4.5 and 6 kb (9). IKK-1 and IKK-2 mRNAs were expressed in Jurkat, HeLa, and HUVEC cell lines, and their amounts were not altered for up to 8 hours after stimulation of cells with TNF-α (HeLa and HUVEC) or antibody to CD28 plus PMA (Jurkat) (9).

Immunoprecipitates of epitope-tagged IKK-1 and IKK-2, expressed in rabbit reticulocyte lysates (RRLs) (20), phosphorylated IκB-α and IκB-β (Fig. 4A). IKK-1 autophosphorylated (Fig. 4A), whereas a kinase-inactive version of IKK-1, in which the conserved Lys[44] was mutated to Met (K44M), showed no autophosphorylation (9). IKK-2, although expressed in equivalent amounts in the lysates, showed very weak autophosphorylation. Immunoprecipitates of either IKK-1 or IKK-2 phosphorylate the IκB-α (21–41) peptide and two different IκB-α (21–41) peptides, each bearing an unmodified Ser at position 32 or 36 and P-Ser at the other position (Fig. 4B). IKK-1 and IKK-2, therefore, can independently phosphorylate both Ser[32] and Ser[36].

Regulation of recombinant IKK-1 and IKK-2 activity, overexpressed in HeLa cells, appeared markedly different. Immunoprecipitates containing recombinant IKK-1 were inactive unless the cells were stimulated (Fig. 4C). In contrast, IKK-2 immunoprecipitates yielded strong constitutively active IκB kinase activity in the absence of cell stimulation. However, immunoprecipitates containing the endogenous IKKs were inactive unless the cells had been stimulated (Fig. 4D). Interestingly, both IKK-1 and IKK-2 contain a canonical MAP kinase kinase (MAPKK) activation loop motif (Ser-Xaa-Xaa-Xaa-Ser, where Xaa is any amino acid) (Fig. 3A). Phosphorylation of both Ser residues is necessary for activation of MAPKK (*21*). We generated IKK-2 mutants in which Ser[177] and Ser[181] were mutated to Ala or Glu (S177A, S181A or S177E, S181E) to block or mimic, respectively, the effect of P-Ser. When expressed in RRL, IKK-2 (S177E, S181E) generated a highly active IκB-α kinase activity (Fig. 4E). The corresponding IKK-1 (S176E, S180E) mutation minimally enhanced kinase activity (9).

Both IKK proteins appear to have roles in NF-κB activation, although our data indicate that IKK-2 is more active. Immunocytochemical studies (*22*) showed that IKK-2 K44M and IKK-2 (S177A, S181A) mutants had no effect on subcellular localization of RelA in unstimulated HeLa cells. However, both mutants inhibited RelA nuclear translocation in TNF-α–stimulated cells (Fig. 5A). The corresponding IKK-1 mutants, expressed at approximately equivalent amounts, had little inhibitory activity (Fig. 5A). The effects of the IKK-1 and IKK-2 mutants on NF-κB–dependent gene expression (Fig. 5B) paralleled those observed in the immunocytochemical studies (Fig. 5A). Both IKK-2 K44M and IKK-2 (S177A, S181A) inhibited TNF-α–stimulated NF-κB–mediated gene activation, whereas IKK-2 (S177E, S181E) induced activity in the absence of cell stimulation (Fig. 5B). Expression of IKK-1 mutants also perturbed NF-κB–mediated gene expression, although the effects were not as pronounced as for the IKK-2 mutants.

The IKK family of serine protein kinases

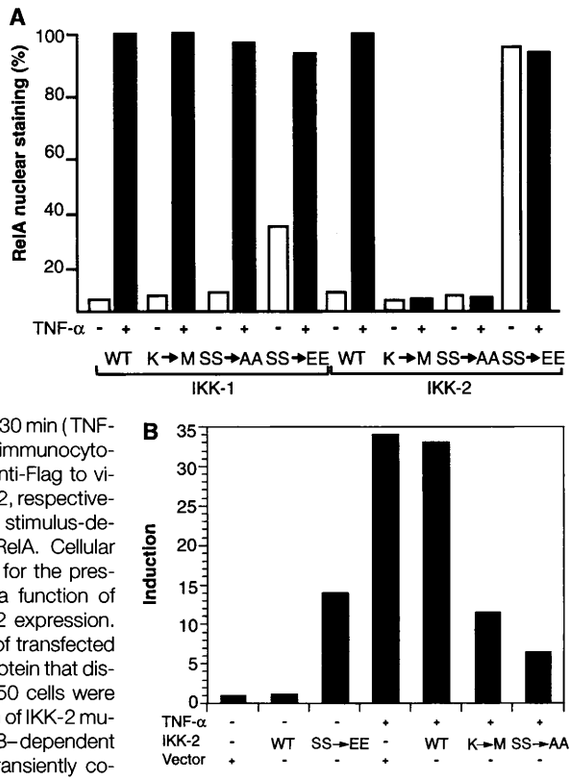

Fig. 5. IKK-2 mediates an essential step in the NF-κB activation pathway. (**A**) IKK-2 mutants block stimulus-dependent RelA nuclear translocation. HeLa cells were transiently transfected with functionally equivalent mutants of either HA-tagged IKK-1 or Flag-tagged IKK-2 as indicated [HA-tagged IKK-1 WT, K44M (K→M), (S176A, S180A) (SS→AA), (S176E, S180E) (SS→EE); Flag-tagged IKK-2 WT, K44M (K→M), (S177A, S181A) (SS→AA), (S177E, S181E) (SS→EE)]. Thirty-six hours after transfection, cells were not stimulated or were stimulated with TNF-α (20 ng/ml) for 30 min (TNF-α). Cells were then subjected to immunocytochemical analysis with anti-HA or anti-Flag to visualize expression of IKK-1 and IKK-2, respectively. Anti-RelA were used to monitor stimulus-dependent nuclear translocation of RelA. Cellular immunofluorescence was analyzed for the presence of RelA nuclear staining as a function of either WT or mutant IKK-1 or IKK-2 expression. Data are presented as percentage of transfected cells expressing the indicated IKK protein that display clear RelA nuclear staining; >50 cells were scored per treatment. (**B**) Expression of IKK-2 mutants has a marked effect on NF-κB–dependent gene activation. HeLa cells were transiently cotransfected with a 3× NF-κB luciferase reporter vector and either an empty control vector or an IKK-2 expression vector as indicated. Thirty-six hours after transfection cells were not stimulated or were stimulated with TNF-α (20 ng/ml) for 5 hours before harvesting. Luciferase activities were determined and normalized on the basis of β-galactosidase activity. Average induction (fold) of luciferase activity was determined from a representative transfection experiment done in duplicate.

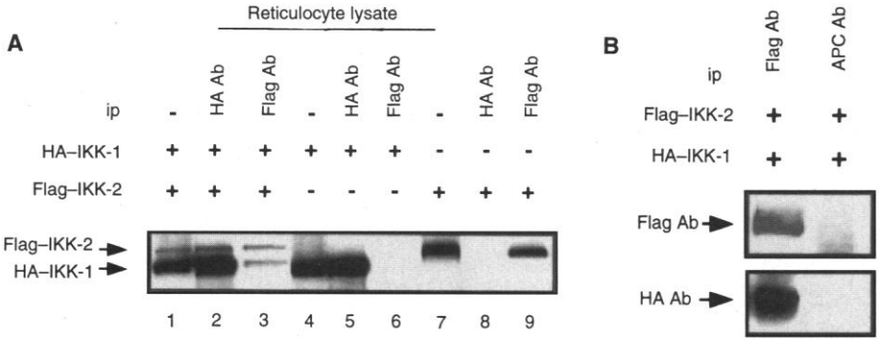

Fig. 6. Interaction between IKK-1 and IKK-2. (**A**) IKK-1 and IKK-2 coprecipitate when translated in RRLs. HA-tagged IKK-1 and Flag-tagged IKK-2 were translated in vitro in RRLs either separately or in combination. The programmed translation mixture was then subjected to immunoprecipitation with the indicated antibody. Samples were subjected to SDS-PAGE and autoradiography. (**B**) IKK-1 and IKK-2 coprecipitate when coexpressed in HeLa cells. HeLa cells were transiently cotransfected with HA-tagged IKK-1 and Flag-tagged IKK-2. Thirty-six hours after transfection, cells were harvested and WCEs were prepared. Lysates were then immunoprecipitated with anti-flag or anti-APC (adenomatous polyposis coli). The immunocomplex was subjected to SDS-PAGE and protein immunoblotting with anti-HA or anti-Flag as indicated on the left.

are unique in that they contain both a leucine zipper and a helix-loop-helix interaction motif. We examined both in vitro and in vivo whether IKK-1 and IKK-2 form stable heterodimers. Influenza virus hemagglutinin (HA) epitope-tagged IKK-1 and Flag (IBI-Kodak) epitope-tagged IKK-2 were translated in RRLs, either alone or together, and then immunoprecipitated (Fig. 6A). IKK-2 was present in IKK-1 immunoprecipitates and vice versa. Heterodimerization appears to be favored over homodimerization, because IKK-1 and IKK-2, when expressed separately and then combined, quantitatively form heterodimers (9). IKK-1 and IKK-2 also coimmunoprecipitate when coexpressed in HeLa cells (Fig. 6B). Removal of the leucine zipper and helix-loop-helix interaction motifs abrogated heterodimerization (9).

The IκB kinase responsible for the initial and critical step of NF-κB activation has been the subject of intense interest. Many kinases have been proposed as candidates (*23*), but only the recently described CHUK IKK-α (*24*), which we refer to as IKK-1, has the characteristics expected of a cytokine-inducible IκB kinase. We have identified IKK-1 and the closely related kinase IKK-2 as interacting components of the IKK signalsome, a multiprotein signaling complex that regulates NF-κB activation in response to proinflammatory cytokines. Our results strongly suggest that IKK-1 and IKK-2 are functional kinases within the IKK signalsome that mediate IκB phosphorylation and NF-κB activation. As a protein complex containing multiple interacting components, including a RelA kinase, the IKK signalsome has the potential to integrate the diverse signaling pathways known to activate NF-κB in different cell types and channel them toward selective gene expression. Drugs that modulate the activation and function of the IKK signalsome are likely to have therapeutic value in inflammatory and neurodegenerative diseases as well as in cancer.

REFERENCES AND NOTES

1. I. M. Verma, J. K. Stevenson, E. M. Schwarz, D. Van Antwerp, S. Miyamoto, *Genes Dev.* **9**, 2723 (1995); P. Baeuerle and T. Henkel, *Annu. Rev. Immunol.* **12**, 141 (1994); A. Manning, *Drug Discovery Today* **1**, 151 (1996); P. J. Barnes and M. Karin, *N. Engl. J. Med.* **336**, 1066 (1997); P. A. Baeuerle and D. Baltimore, *Cell* **87**, 13 (1996); V. R. Baichwal and P. A. Baeuerle, *Curr. Biol.* **7**, 94 (1997).
2. P. A. Baeuerle and D. Baltimore, *Cell* **53**, 211 (1988); ———, *Genes Dev.* **3**, 1689 (1989).
3. J. E. Thompson, R. J. Philips, H. Erdjument-Bromage, P. Tempst, S. Ghosh, *Cell* **80**, 573 (1995); Z. Cao, W. Henzel, X. Gao, *Science* **271**, 1128 (1996); U. Siebenlist, G. Franzoso, K. Brown, *Annu. Rev. Cell Biol.* **10**, 405 (1994).
4. A. A. Beg and A. S. Baldwin Jr., *Genes Dev.* **7**, 2064 (1993); T. D. Gilmore and P. J. Morin, *Trends Genet.* **9**, 427 (1993); M. T. Diaz-Meco *et al.*, *Mol. Cell. Biol.* **13**, 4770 (1993); S. Haskill *et al.*, *Cell* **65**, 1281 (1991).
5. A. A. Beg *et al.*, *Genes Dev.* **6**, 1899 (1992); I. Alkalay *et al.*, *Mol. Cell. Biol.* **15**, 1294 (1995); J. A. DiDonato, F. Mercurio, M. Karin, *ibid.*, p. 1302 (1995); A. Hershko and A. Ciechanover, *Annu. Rev. Biochem.* **61**, 761 (1992); D. C. Scherer, J. Brockman, Z. Chen, T. Maniatis, D. Ballard, *Proc. Natl. Acad. Sci. U.S.A.* **92**, 11259 (1995); M. Roff *et al.*, *J. Biol. Chem.* **271**, 7844 (1996).
6. K. Brown, S. Gerstberger, L. Carlson, G. Franzoso, U. Siebenlist, *Science* **267**, 1485 (1995); E. B. M. Traenckner *et al.*, *EMBO J.* **14**, 2876 (1995); S. T. Whiteside *et al.*, *Mol. Cell. Biol.* **15**, 5339 (1995); J. A. DiDonato *et al.*, *ibid.* **16**, 1295 (1996).
7. HeLa S3 cells were harvested and resuspended in two packed cell pellet volumes of WCE lysis buffer [20 mM tris-HCl (pH 8.0), 0.5 M NaCl, 0.25% Triton X-100, 1 mM EDTA, 1 mM EGTA, 10 mM β-glycerophosphate, 10 mM NaF, 10 mM 4-nitrophenyl phosphate (PNPP), 300 μM Na_3VO_4, 1 mM benzamidine, 2 μM phenylmethylsulfonyl fluoride (PMSF), aprotinin at 10 μg/ml, leupeptin at 1 μg/ml, pepstatin at 1 μg/ml, 1 mM dithiothreitol (DTT)], and gently rotated at 4°C for 45 min; the lysate was centrifuged at 60,000 rpm for 60 min in a Ti50.1 rotor at 4°C. The supernatant was dialyzed into 50 mM Q buffer [20 mM tris-HCl (pH 8.0), 50 mM NaCl, 0.5 mM EDTA, 0.5 mM EGTA, 0.025% Brij 35, 10 mM β-glycerophosphate, 10 mM NaF, 10 mM PNPP, 300 μM Na_3VO_4, aprotinin at 10 μg/ml, leupeptin at 1 μg/ml, pepstatin at 1 μg/ml, 1 mM DTT] and chromatographed on a Mono Q column (Pharmacia). Mono Q fractions containing IκB-α kinase activity were pooled, concentrated, and fractionated on a Superdex 200 gel-filtration column (Pharmacia). Fractions containing IκB-α kinase activity were pooled and directly fractionated on a Mono Q column. Fractions containing IκB-α kinase activity were pooled and fractionated on a phenyl Superose (Pharmacia) column equilibrated with PS buffer [20 mM tris-HCl (pH 8.0), 0.25 mM EDTA, 0.25 mM EGTA, 1.2 M ammonium sulfate, 10 mM β-glycerophosphate, 10 mM NaF, 10 mM PNPP, 300 μM Na_3VO_4, 1 mM benzamidine, 2 μM PMSF, aprotinin at 10 μg/ml, leupeptin at 1 μg/ml, pepstatin at 1 μg/ml, 1 mM DTT], and the kinase was eluted in a gradient to PS buffer with no ammonium sulfate. Fractions containing IκB kinase activity were subjected to immunoblot analysis with anti-RelA, anti–IκB-β, and anti–MKP-1 (Santa Cruz Biotechnology, Inc.) or anti–MEKK-1 or anti–P-Tyr (Upstate Biotechnology).
8. IKK signalsome kinase assay. Samples from column fractions or immunoprecipitates were subjected to an in vitro kinase assay. Kinase assays were done in kinase buffer [20 mM Hepes (pH 7.7), 2 mM $MgCl_2$, 2 mM $MnCl_2$, 10 μM adenosine triphosphate (ATP), 1 to 3 μCi of [γ-^{32}P]ATP, 10 mM β-glycerophosphate, 10 mM NaF, 10 mM PNPP, 300 μM Na_3VO_4, 1 mM benzamidine, 2 μM PMSF, aprotinin at 10 μg/ml, leupeptin at 1 μg/ml, pepstatin at 1 μg/ml, 1 mM DTT] at 30°C for 30 to 60 min in the presence of the indicated substrate. The kinase reaction was stopped by addition of 6× SDS–polyacrylamide gel electrophoresis (PAGE) sample buffer, subjected to SDS-PAGE analysis, and visualized by autoradiography. GST–IκB substrates were expressed and purified from *Escherichia coli* with glutathione Sepharose 4B beads. His-tagged RelA–streptavidin-tagged IκB-α WT and His-tagged Rel A–streptavidin-tagged IκB-α (S32A, S36A) mutant complexes were purified from Sf9 cells coinfected with the indicated baculoviral expression constructs.
9. F. Mercurio, B. Bennett, B. Murray, L. Ransone, H. Zhu, A. Manning, unpublished data.
10. Z. J. Chen, L. Parent, T. Maniatis, *Cell* **84**, 853 (1996).
11. F. S. Lee, J. Hagler, Z. J. Chen, T. Maniatis, *ibid.* **88**, 213 (1997); M. Hirano *et al.*, *J. Biol. Chem.* **271**, 13234 (1996); N. L. Malinin, M. P. Bolin, A. V. Kovalenko, D. Wallach, *Nature* **385**, 540 (1997).
12. Two 150-mm plates of HeLa cells were either stimulated with TNF-α or not; whole-cell lysates were prepared and diluted with 3 vol of PD buffer [40 mM tris-HCl (pH 8.0), 500 mM NaCl, 0.1% Nonidet P-40, 6 mM EDTA, 6 mM EGTA, 10 mM β-glycerophosphate, 10 mM NaF, 10 mM PNPP, 300 μM Na_3VO_4, 1 mM benzamidine, 2 μM PMSF, aprotinin at 10 μg/ml, leupeptin at 1 μg/ml, pepstatin at 1 μg/ml, 1 mM DTT]; 2 to 4 μg of the indicated antibody was added, and samples were incubated on ice for 1 to 2 hours. Protein A or G beads (10 μl) were added and samples were incubated for 1 hour at 4°C. The immunoprecipitate was then washed three times with PD buffer and once with kinase buffer without ATP and then subjected to a standard kinase assay. There was no loss in IκB kinase activity when the immunoprecipitate was subjected to more rigorous washing—RIPA buffer [50 mM tris-HCl (pH 8.0), 150 mM NaCl, 1 mM EDTA, 0.4% deoxycholate, 1% Nonidet P-40, 10 mM β-glycerophosphate, 10 mM NaF, 10 mM PNPP, 300 μM Na_3VO_4, 1 mM benzamidine, 2 μM PMSF, aprotinin at 10 μg/ml, leupeptin at 1 μg/ml, pepstatin at 1 μg/ml, 1 mM DTT] or up to 3.5 M urea.
13. Peptide phosphorylation was done as described (*8*) with synthetic peptides (100 μM) (Alpha Diagnostics International, San Antonio, TX). Reactions were for 1 hour at room temperature and were terminated by the addition of SDS-PAGE loading buffer. SDS-PAGE with a 16% tris Tricine gel (Novex) or a 4 to 20% tris glycine gel (Novex) was used to characterize the reaction products. Gels were washed, dried in vacuo, and exposed to autoradiographic film. Peptide sequences were as follows: IκB-α (21–41), CK-KERLLDDRHDSGLDSMKDEE; IκB-α (21–41) S→T mutant, CKKERLLDDRHDTGLDTMKDEE; c-Fos (222–241), DLTGGPEVAT(PO_3)PESEEAFLP; MKP-1, CPTNSALNYLKSPITTSPS; c-Jun (56–70), CNS-DLLTSPDVGLLK; c-Jun (65–79), CVGLLKLASPEL-ERL. Abbreviations for amino acid residues are as follows: A, Ala; C, Cys; D, Asp; E, Glu; F, Phe; G, Gly; H, His; I, Ile; K, Lys; L, Leu; M, Met; N, Asn; P, Pro; Q, Gln; R, Arg; S, Ser; T, Thr; V, Val; W, Trp; Y, Tyr. Incorporation of ^{32}P into GST–IκB-α (1–54) was measured in a discontinuous assay as described above (*8*). GST–IκB-α (1–54) and ATP were 0.56 and 3 μM, respectively. Enzymatic reactions (32 μl) were carried out for 1 hour at room temperature and terminated with the addition of trichloroacetic acid (TCA) (150 μl per well; 12.5%, w/v). After 20 min, the TCA precipitate was collected on 96-well glass fiber plates (Packard) and washed 10 times with about 0.3 ml of Dulbecco's phosphate-buffered saline (pH 7.4) per well (Sigma). Scintillation fluid (0.50 ml; MicroScint, Packard) was added to each well and ^{32}P was detected by scintillation counting. Less than 10% of the ATP was consumed in the reaction.
14. For large-scale IKK signalsome purification, HeLa S3 cells were stimulated for 7 min with TNF-α at 20 ng/ml (R&D Systems) and harvested; whole-cell lysate was prepared (1.2 g of total protein) and about 5 mg of anti–MKP-1 (Santa Cruz Biotechnology, Inc.) was added and incubated at 4°C for 2 hours with gentle rotation. Then 50 ml of protein A–agarose (Calbiochem) was added and incubated for 2 hours. The immunoprecipitate was then sequentially washed four times with PD buffer, two times with RIPA buffer, two times with PD buffer, once with 3.5 M urea-PD buffer, and three times with PD buffer. The immunoprecipitate was then made into a thick slurry by adding 10 ml of PD buffer and 25 mg of the MKP-1 peptide to which the antibody was generated (Santa Cruz Biotechnology, Inc.); then it was incubated overnight at 4°C with gentle rotation. Salt was removed from the eluted protein on PD10 columns (Pharmacia) equilibrated with 50 mM Q buffer, and eluate was chromatographed on a Mono Q column (Pharmacia). Fractions containing IκB kinase activity were pooled, concentrated, and subjected to preparative SDS-PAGE; protein bands were visualized with colloidal blue stain (Novex) and the bands were excised and sequenced.
15. Coomassie blue–stained bands were excised and digested with trypsin as described. A small portion of the supernatant was removed for analysis by MALDI peptide mapping as described (*16*). The program PeptideSearch (EMBL, Heidelberg) was used to compare the peptide mass map from the IKK-1 band with a protein sequence database. Eight measured peptide masses matched those calculated for peptides from CHUK within 30 ppm (*18*). The peptide mass map of the IKK-2 band did not result in a clear identification and therefore the sample was subject-

ed to nanoelectrospray mass spectrometry (25). The peptide mixture was micropurified on a capillary containing 50 nl of Poros R2 resin (Perseptive Biosystems, Framingham, MA). The peptides were washed and then step-eluted with 0.5 μl of 50% MeOH in 5% formic acid into a nanoelectrospray needle. This needle was transferred to an APIII mass spectrometer (Perkin-Elmer, Sciex, Toronto, Canada) and the sample was sprayed for about 20 min. During this time, peptide ions apparent from the mass spectrum were selected and isolated and then fragmented in the collision chamber of the mass spectrometer. From the tandem mass spectra, short stretches of sequence were assembled into peptide sequence tags (18) and compared with a protein sequence database or an EST database by using PeptideSearch. Three peptides matched the IKK-1 sequence. A1, IIDLGYAK; A2, VEVALSNIK; A3, SIQLDLER. Three other peptides matched human EST sequences in the EST database: B1, ALELLPK; B2, VIYTQLSK; B6, LLLQAIQSFEK. These three sequences all match EST clone AA326115. The peptide B4 with the sequence LGTGGFGNVIR was found in clone R06591. After the full-length IKK-2 sequence was obtained (19), two more peptides (B3, ALDDILNLK; B5, DLKPENIVLQQGEQR) were found in the sequence. Peptide A1 is present in both IKK-1 and IKK-2 sequences.

16. A. Shevchenko *et al.*, *Proc. Natl. Acad. Sci. U.S.A.* **93**, 14440 (1996).
17. M. A. Connely and K. B. Marcu, *Cell. Mol. Biol. Res.* **41**, 537 (1995).
18. M. Mann and M. S. Wilm, *Anal. Chem.* **66**, 4390 (1994); M. Wilm *et al.*, *Nature* **379**, 466 (1996); M. Mann, *Trends Biol. Sci.* **21**, 494 (1996).
19. Several peptides were identical matches to human EST clones. All the EST clones were similar to human and mouse CHUK-1 (IKK-1). These clones were obtained (Genome Systems, Inc.) and the precise nucleotide sequence was determined and used to design primers to clone human IKK-2 by polymerase chain reaction (PCR) from a human HeLa cell cDNA library (Clontech, Inc.). Several IKK-2 cDNA clones were isolated and sequenced. Full-length mouse IKK-1 and a partial human IKK-1 nucleotide sequence were available in the comprehensive database. Primers were designed to clone by PCR the human and mouse IKK-1 cDNAs. The partial human IKK-1 coding region was used to probe a HeLa cDNA phage library (Stratagene) to obtain the full-length human IKK-1 cDNA clone by standard procedures.
20. For in vitro translation studies, HA-tagged IKK-1 and Flag-tagged IKK-2 were in vitro translated in RRLs, either separately or alone, exactly as described in the manufacturer's protocol (Promega).
21. C.-F. Zheng and K.-L. Guan, *EMBO J.* **13**, 1123 (1994).
22. For immunocytochemistry, HeLa cells were transiently transfected with either HA-tagged IKK-1 or Flag-tagged IKK-2 as indicated. Cells were washed with PBS, fixed with 4% paraformaldehyde (Electron Microscopy Sciences) for 30 min, and permeabilized with wash buffer (0.5% Triton X-100, 0.01% azide in PBS). Cells were blocked with wash buffer containing donkey serum (5%) (Jackson Immunoresearch Laboratories) and probed with primary antibody—anti-RelA (polyclonal antibody), 1:2000 (Santa Cruz); anti-HA (monoclonal antibody), 1:1000 (Eastman Kodak); or anti-Flag (monoclonal antibody), 1:1000 (Babco)—followed by secondary antibody—donkey antibody to rabbit (fluorescein isothiocyanate) conjugate, 1:100; donkey antibody to mouse (Texas Red conjugate), 1:100 (Jackson Immunoresearch Laboratories). Cover slips were mounted with polyvinyl alcohol and 1,4-diazabicyclo[2.2.2]octane (Sigma) mounting medium and the slides were viewed under fluorescence with a Nikon Microphot-FXA microscope; the images were then scored and photographed.
23. A. Kumar, J. Haque, J. Lacoste, J. Hiscott, B. R. G. Williams, *Proc. Natl. Acad. Sci. U.S.A.* **91**, 6288 (1994); M. T. Diaz-Meco *et al.*, *Mol. Cell. Biol.* **13**, 4770 (1993); M. T. Diaz-Meco *et al.*, *EMBO J.* **13**, 1842 (1994); G. J. Schouten *et al.*, *ibid.* **16**, 3133 (1997).
24. J. A. DiDonato, M. Hayakawa, D. M. Rothwarf, E. Zandi, M. Karin, *Nature* **388**, 548 (1997); C. H. Regnier *et al.*, *Cell* **90**, 373 (1997).
25. M. Wilm and M. Mann, *Anal. Chem.* **68**, 1 (1996).

26. We thank I. Verma and R. Mueller for the gift of the IκB-α COOH-terminus construct and helpful discussions; J. DiDonato for the IκB-α vectors; H. Raymon and N. Richard for assistance with immunocytochemistry; S. Kim, A. LaPointe, and B. Lee for technical assistance; K. Davis and E. Carlson for help with compiling the manuscript and figures; and D. Anderson and A. Lewis for helpful comments and support. A.R. contributed to this work during a sabbatical at Signal Pharmaceuticals.

22 July 1997; accepted 15 September 1997

IκB Kinase–β: NF-κB Activation and Complex Formation with IκB Kinase–α and NIK

John D. Woronicz, Xiong Gao, Zhaodan Cao, Mike Rothe, David V. Goeddel*

Activation of the transcription factor nuclear factor kappa B (NF-κB) by inflammatory cytokines requires the successive action of NF-κB–inducing kinase (NIK) and IκB kinase–α (IKK-α). A widely expressed protein kinase was identified that is 52 percent identical to IKK-α. IκB kinase–β (IKK-β) activated NF-κB when overexpressed and phosphorylated serine residues 32 and 36 of IκB-α and serines 19 and 23 of IκB-β. The activity of IKK-β was stimulated by tumor necrosis factor and interleukin-1 treatment. IKK-α and IKK-β formed heterodimers that interacted with NIK. Overexpression of a catalytically inactive form of IKK-β blocked cytokine-induced NF-κB activation. Thus, an active IκB kinase complex may require three distinct protein kinases.

Transcriptional activation of inflammatory response genes by tumor necrosis factor (TNF), interleukin-1 (IL-1), and other external stimuli is mediated by the transcription factor NF-κB (*1*, *2*). Normally, NF-κB is held in an inactive state in the cytoplasm by IκB inhibitory proteins. When cells are treated with TNF or IL-1, protein kinase cascades are activated that lead to phosphorylation of IκB proteins on two specific serine residues (*1*, *2*). This signal-induced phosphorylation targets IκB for ubiquitination and proteosome-mediated degradation, allowing nuclear translocation of NF-κB (*2*).

Several steps of the TNF- and IL-1–activated signaling pathways leading to IκB phosphorylation have now been elucidated (*3*–*10*). Both pathways merge at the level of the protein kinase NIK (NF-κB–inducing kinase) (*10*). The molecular mechanisms by which NIK becomes activated are not yet understood. However, the protein kinase CHUK is a downstream target of NIK (*11*) that directly associates with IκB-α and specifically phosphorylates it on serines 32 and 36 (*11*, *12*). These results have led to the redesignation of CHUK as IκB kinase–α (IKK-α).

IKK-α does not phosphorylate the two serines required for degradation of a second member of the IκB family, IκB-β, with equal efficiency; it has a marked preference for serine 23 over serine 19 (*11*). This finding indicates that another kinase might be responsible for IκB-β phosphorylation. Furthermore, mapping of the gene encoding CHUK revealed the presence of a CHUK-related sequence in the mouse genome (*13*). To search for IKK-α–related kinases, we screened the National Center for Biotechnology Information DNA database and identified an expressed sequence tag (EST) cDNA clone predicted to encode a polypeptide 57% identical to amino acids 624 to 658 of IKK-α (*14*). Full-length human cDNAs corresponding to the EST sequence were isolated from a Jurkat T cell cDNA library and found to encode a 756–amino acid protein very similar to IKK-α, which we designate IKK-β (Fig. 1). Overall, the sequences of IKK-α and IKK-β are 52% identical, with the NH_2-terminal kinase domains sharing 64% identity and the COOH-terminal regions, which contain leucine zipper and helix-loop-helix domains, having 44% sequence identity. An IKK-β mRNA of ~3.8 kb was detected by Northern (RNA) blot analysis in all tissues examined (*15*).

To determine whether IKK-β might have a role in NF-κB activation, we compared the ability of IKK-α and IKK-β to activate an NF-κB–dependent reporter gene in transiently transfected 293 cells (*16*). Overexpression of IKK-β gave consistently greater activation of the NF-κB reporter than did IKK-α at equivalent expression levels (Fig. 2A). A catalytically inactive mutant of IKK-β, IKK-$β_{(K44A)}$, failed to activate the NF-κB–dependent reporter gene when overexpressed and inhibited both TNF- and IL-1–induced NF-κB activation in a dose-dependent manner (Fig. 2B). In constrast, overexpression of wild-type IKK-β further enhanced TNF- and

Tularik, Two Corporate Drive, South San Francisco, CA 94080, USA.

*To whom correspondence should be addressed. E-mail: goeddel@tularik.com